ORIGINAL ARTICLE

Calibration of SARRA-H model for climatic risk zoning of cowpea in Eastern Amazon[1]

Calibração do modelo SARRA-H para o zoneamento de risco climático do caupi na Amazônia Oriental

Paulo J. O. P. Souza[2]*, João V. de N. Pinto[3], Hildo G. G. C. Nunes[4], Everaldo B. de Souza[5], Alailson V. Santiago[6], Gabriel S. T. Fernandes[2], Matheus L. Rua[2], Vivian D. da S. Farias[7] & Denis de P. Sousa[8]

[1] Research developed at School Farm of the Universidade Federal Rural da Amazônia, Castanhal, Pará, Brazil
[2] Universidade Federal Rural da Amazônia, Belém, PA, Brazil
[3] Instituto Federal de Educação, Ciência e Tecnologia do Amapá, Campus Porto Grande, Porto Grande, AP, Brazil
[4] Secretária de Estado de Meio Ambiente e Sustentabilidade/Núcleo de Monitoramento Hidrometeorológico, Belém, PA, Brazil
[5] Universidade Federal do Pará/Instituto de Geociências, Belém, PA, Brazil
[6] Embrapa Amazônia Oriental, Belém, PA, Brazil
[7] Universidade Federal do Pará/Campus Altamira/Faculdade de Engenharia Agronômica, Altamira, PA, Brazil
[8] Secretária de Estado de Meio Ambiente e Sustentabilidade/Diretoria de Fiscalização Ambiental, Belém, PA, Brazil

HIGHLIGHTS:
The SARRA-H crop model can simulate cowpea phenology and yield in Eastern Amazon.
Cowpea production in the Eastern Amazon is impacted by water deficit and high incidence of rain during the harvest period.
The northern half of the studied region has optimal conditions for the growth, development and harvesting of cowpea.

ABSTRACT: This study aimed to calibrate and test the SARRA-H (Système d'Analyse Régionale des Risques Agroclimatologiques) crop model for cowpea, as well as conducting a climate risk zoning for this crop in a region located in Eastern Amazon, allowing the identification of locations and sowing dates that favor the production considering both the water deficit and the probability of occurrence of severe rains during the harvest period. The model was calibrated and validated with data from experiments conducted between 2013 and 2016 in the municipality of Castanhal, PA, Brazil. Low climate risk areas were defined as those that had a water requirement satisfaction index (WRSI) greater than or equal to 0.5 in the reproductive phase combined with the occurrence of rainfall below 20 mm at the harvest for, at least, 80% of the years for which planting was simulated. The model was able to simulate the water balance, growth and development of cowpea under the climate and soil conditions of the studied location with high precision and accuracy. The optimal period for sowing cowpea comprises the interval between June 5th and 25th for regions located above 2° S and between March 25th and April 15th for regions below 2° S.

Key words: *Vigna unguiculata*, water requirement satisfaction index, yield, climate risk management

RESUMO: Esta pesquisa teve como objetivo calibrar e testar o modelo de cultura SARRA-H (Système d'Analyse Régionale des Risques Agroclimatologiques) para o caupi, bem como realizar o zoneamento de risco climático para esta cultura em uma região localizada na Amazônia Oriental, a fim de permitir a identificação de locais e datas de semeadura que favoreçam a produção considerando tanto o déficit hídrico como a probabilidade de ocorrência de chuvas severas durante o período da colheita. O modelo foi calibrado e validado com dados de experimentos realizados entre 2013 e 2016 no município de Castanhal, PA. As áreas de baixo risco climático foram definidas como aquelas que apresentaram índice de satisfação da necessidade hídrica (WRSI) maior ou igual a 0,5 na fase reprodutiva combinado com a ocorrência de chuvas abaixo de 20 mm na colheita por, pelo menos, 80% dos anos onde foi simulado o plantio. O modelo foi capaz de simular o balanço hídrico, crescimento e desenvolvimento do feijão-caupi nas condições climáticas e de solo da região estudada com boa precisão e exatidão. O período de ótima semeadura para o feijão-caupi compreende o intervalo entre 5 e 25 de junho para regiões localizadas acima de 2° S, e entre 25 de março e 15 de abril para regiões abaixo de 2° S.

Palavras-chave: *Vigna unguiculata*, índice de satisfação das necessidades de água, produtividade, manejo de risco climático

Introduction

Cowpea (*Vigna unguiculata* (L.) Walp) was introduced in Brazil by colonizers, becoming an important crop for small producers in the North and Northeast of Brazil. Although different studies indicate that the potential yield for cowpea in the country can exceed 1,500 kg ha^{-1} (Machado et al., 2008), the average yield in Pará state, Brazil, is as low as 821 kg ha^{-1} (Carvalho et al., 2022). The low yield is due to several factors, such as incorrect seed management, inadequate soil fertility, and adverse weather conditions, such as droughts (Sousa et al., 2022).

Studies with proper management, when the climate is the main factor determining crop yield, are conducted using agrometeorological models for climate risk assessment (Yang et al., 2023), which includes climate risk based on the water requirement of the plant (Nunes et al., 2019).

The northeast of Pará state, Brazil, concentrates most of the cowpea production in the state. According to studies, when the accumulated water deficit during the reproductive phase exceeds 47 mm, yield losses of more than 20% may occur (Souza et al., 2020). The excessive rainfall during harvesting may favor the development of several fungal diseases such as the brown blotch, the leaf smut disease, and the *Choenophora* pod rot, which reduces the yield (Benchimol et al., 2021). Therefore, scientific research aimed at estimating the climate risk such as this one would benefit farmers in the region and reduce the uncertainty regarding the production of cowpea.

This study aimed to calibrate and test the SARRA-H model and conduct the climate risk zoning of this crop for the referred region, allowing the identification of locations and sowing dates that favor the production considering both the water deficit and the probability of occurrence of severe rains during the harvest period.

Material and Methods

Field experiments were conducted at the School Farm of the Federal Rural University of Amazon, in the municipality of Castanhal, Pará state, Brazil (1° 19′ 14.7″ S; 47° 57′ 33.5″ W; 41 m of altitude) during the years 2013, 2014, 2015, and 2016. The SARRA-H model was calibrated and validated before its use in climate risk zoning, with the data obtained in the experiments referred to above. In these experiments, cowpea was subjected to different irrigation depths and cultivated with a spacing of 0.5 m between rows and 0.1 m between plants, which totalizes 200,000 plants ha^{-1} of the cultivar BR3-Tracateua, with a cycle of 65-70 days. Fertilization was performed according to the soil chemical analysis, applying 350 kg ha^{-1} of mineral fertilizer with NPK formulation 10-20-20 for the 2015 experiment, and 195 kg ha^{-1} of mineral fertilizer with NPK formulation 6-18-15 for the 2016 experiment.

An experiment was conducted in randomized block design with six blocks of 3 m x 10 m and four treatments (L$_1$, L$_2$, L$_3$, and L$_4$), which corresponded to different irrigation managements during the reproductive phase, as follows. The irrigation depth in L$_1$ replaced 100% of the maximum crop evapotranspiration. The irrigation depth in L$_2$ and L$_3$ corresponded to 50 and

25% of the maximum evapotranspiration, respectively. The irrigation depth in L$_4$ corresponded to 0% of the maximum evapotranspiration, i.e., the irrigation stopped at the beginning of the reproductive phase.

The irrigation needed was estimated using the crop evapotranspiration (ET$_c$), calculated as the reference evapotranspiration - ET$_0$ (Allen et al., 2011) times the crop coefficients (K$_c$) obtained by Farias et al. (2017). A drip irrigation system was used, with emitters with a flow rate of 1.03 L h^1 under a service pressure of 50 kPa and spaced 20 cm apart. ET$_0$ was calculated with data from an automated weather station of the Instituto Nacional de Meteorologia (INMET) located 3 km away from the experiment site. Furthermore, a 3 m high tower was placed in the center of the experiment site to monitor meteorological variables.

Every week three plants were sampled in the center of each plot to determine the total biomass of the shoots. Each plant was divided into leaves, stems, flowers, petioles, peduncles, pods, and grains, which were placed in paper bags and dried in an oven at 70 °C until the weight stabilized. Three discs with a diameter of 2 cm were sampled in each plot from different healthy leaves to calculate the specific leaf mass and the leaf area index.

The SARRA-H (Système d'Analyse Régionale des Risques Agroclimatologiques) model integrates three processes: water balance, carbon balance, and phenological development of the crop (CIRAD, 2023). The model uses the specific leaf area (SLA) to calculate the leaf area index (LAI) and then to obtain the fraction of the photosynthetically active radiation (PAR) intercepted by the canopy. The model calculates the potential carbon uptake of the crop as a function of the efficiency of radiation use. The SARRA-H model considers the total plant biomass (BiomTot) and subtracts a fraction of the assimilated biomass to simulate respiration (Resp) (Eq. 1). A water stress coefficient (Cstr) — defined as the ratio of effective transpiration (Tr) to potential transpiration (TrPot) — restricts the potential assimilation (Eq. 2).

$$BiomTot_i = BiomTot_{i-1} + Assim_i - Resp_i \qquad (1)$$

$$Assim_i = Cstr_i \times + AssimPot_i = \frac{Tr_i}{TrPot_i} \times AssimPot_i \quad (2)$$

where:

BiomTot$_i$ - total dry matter on day i;

BiomTot$_{i-1}$ - total dry matter on the day before i;

Assim$_i$ - dry matter assimilated on day i;

Resp$_i$ - dry matter lost through respiration on day i;

Cstr$_i$ - coefficient of reduction of potential assimilation on day i;

AssimPot$_i$ - potential assimilation on day i;

Tr$_i$ - transpiration on day i; and,

TrPot$_i$ - maximum or potential transpiration on day i.

The model represents the soil as a set of water reservoirs that can fill to its maximum capacity (FC). Three distinct reservoirs exist: (I) the surface reservoir; (II) the deep reservoir, and (III) the root reservoir. The water stored in the soil is the

sum of precipitation and irrigation, subtracting the fraction corresponding to surface runoff and deep drainage. The water that exceeds the capacity of the surface reservoir drains to the deep reservoir, and the water that exceeds the deep reservoir is the deep percolation.

The model divides crop evapotranspiration into two components: evaporation and transpiration. Potential evaporation (EvapPot) (Eq. 3) is restricted by the availability of water in the surface layer, while the availability of water in the root reservoir restricts the potential transpiration (Eq. 4).

$$\text{EvaPot} = K_{ce} \times ET_0 \tag{3}$$

$$\text{TrPot} = K_{cp} \times ET_0 \tag{4}$$

where:

EvapPot - potential or maximum evapotranspiration;

ET_0 - reference evapotranspiration;

TrPot - potential or maximum transpiration;

K_{ce} - evaporation coefficient; and,

K_{cp} - transpiration coefficient.

The maximum crop coefficient (K_c) restricts crop evapotranspiration (Eq. 5). In the model, K_{ce} is the coefficient that controls evaporation. It depends on the rate of solar radiation transmitted to the soil (ltr) - which is a function of the canopy cover. Potential transpiration, in turn, is calculated from the consumption index (K_{cp}), where K_{cp} is a function of (1 - ltr) limited by the maximum crop coefficient.

$$ET_c = K_c \times ET_0 = \left(K_{cp} + K_{ce}\right)ET_0 \tag{5}$$

where:

ETc - potential or maximum crop evapotranspiration;

K_c - crop coefficient;

ET_0 - reference evapotranspiration;

K_{cp} - crop coefficient for transpiration; and,

K_{ce} - crop coefficient for evaporation.

Reference evapotranspiration was calculated for each day based on weather records, according to the methodology described by Allen et al. (2011). Table 1 presents the parameters of the SARRA-H model that were adjusted/replaced according to data from the field experiment. The other parameters were left with their original values (CIRAD, 2023).

The water requirement satisfaction index (WRSI) is the ratio of the actual evapotranspiration (ETR) of the crop to its maximum evapotranspiration (ETM) (Andrade Júnior et al., 2007; 2018). The current study considers an average WRSI ≥ 0.5 during the reproductive phase as low water stress.

Data from 24 weather stations of the Instituto Nacional de Meteorologia were used, including automated and conventional stations (Figure 1) limited to the period from 1987 to 2016 (30 years of data).

A validation routine removed inconsistent records of the weather data. Missing data, and values removed by the validation routine, were estimated by interpolation using the inverse distance weighting (IDW) method.

The predominant soil texture at each of the 30 locations was obtained by consulting the map of soils in Pará and Maranhão

**Table 1.** Crop parameters of the SARRA-H crop model and the values used

Parameter	Value	Unity	Description
SDJLevee	101	°C day	Thermal time from sowing until germination.
SDJBVP	506	°C day	Thermal time from germination until the end of the vegetative phase.
SDJRPR	266	°C day	Thermal time from the beginning of flowering until the end of grain growth stage.
SDJMatu1	236	°C day	Thermal time from the beginning until the end of the grain growth stage.
SDJMatu2	182	°C day	Thermal time from the end of grain growth until the harvest.
KRdtPotA	0.1155	kg kg^{-1}	Coefficient to estimate potential crop yield from the total biomass accumulated at the end of flowering.
PPSens	1	-	Photoperiod sensitivity (1 means no sensitivity to photoperiod)
TxConversion[1]	8.3	-	Maximum radiation use efficiency based on total dry matter of the crop.
TxAssimBVP[1]	1	-	Multiplication factor for radiation use efficiency during the vegetative development.
TxAssimMatu1[1]	0.6	-	Multiplication factor for radiation use efficiency during grain growth stage.
TxAssimMatu2[1]	0.5	-	Multiplication factor for radiation use efficiency during grain maturation.
AeroTotBase	0.65	-	Offset of the regression equation of the ratio of aerial to total dry matter as function of total dry matter.
AeroTotPente	0	-	Slope of the regression equation of the ratio of aerial to total dry matter as a function of total dry matter.
FeuilAeroBase	0.57	-	Offset of the regression equation of the ratio of leaves to aerial dry matter as a function of aerial dry matter.
FeuilAeroPente	-5.7E-05	-	Slope of the regression equation of the ratio of leaves to aerial dry matter as a function of aerial dry matter.
KcMax[2]	1.4	-	Maximum crop coefficient.
Kdf[3]	0.77	-	Radiation extinction coefficient.
PoidsSecGrain	0.14	g	Mean dry matter of cowpea grain.
VRacLevee[4]	5	mm per day	Daily deepening of roots during the germination.
VRacBVP[4]	5	mm per day	Daily deepening of roots during the vegetative development.
VRacRPR[4]	15	mm per day	Daily deepening of roots during flowering.
VRacMatu1[4]	10	per day	Daily deepening of roots during the grain growth stage.
VRacMatu2[4]	0	per day	Daily deepening of roots during the maturation.
SlaMin	0.000804	ha kg^{-1}	Initial specific leaf area.
SlaMax	0.00119456	ha kg^{-1}	Final specific leaf area.

[1] Radiation use efficiency was adjusted to be about twice the value of 2.23 found by Sousa et al. (2018) at the end of the crop's lifetime. The radiation use efficiency found by Sousa et al. (2018) was calculated with the aerial dry matter, which is the usual procedure; however, SARRA-H simulations account for the whole plant, so the model's manual states that the input value might be as high as twice the values reported in scientific publications.
[2] Farias et al. (2017).
[3] Mean value reported by Sousa et al. (2018).
[4] Values fitted so that root depth reaches about 30 cm during the reproductive phase of the crop
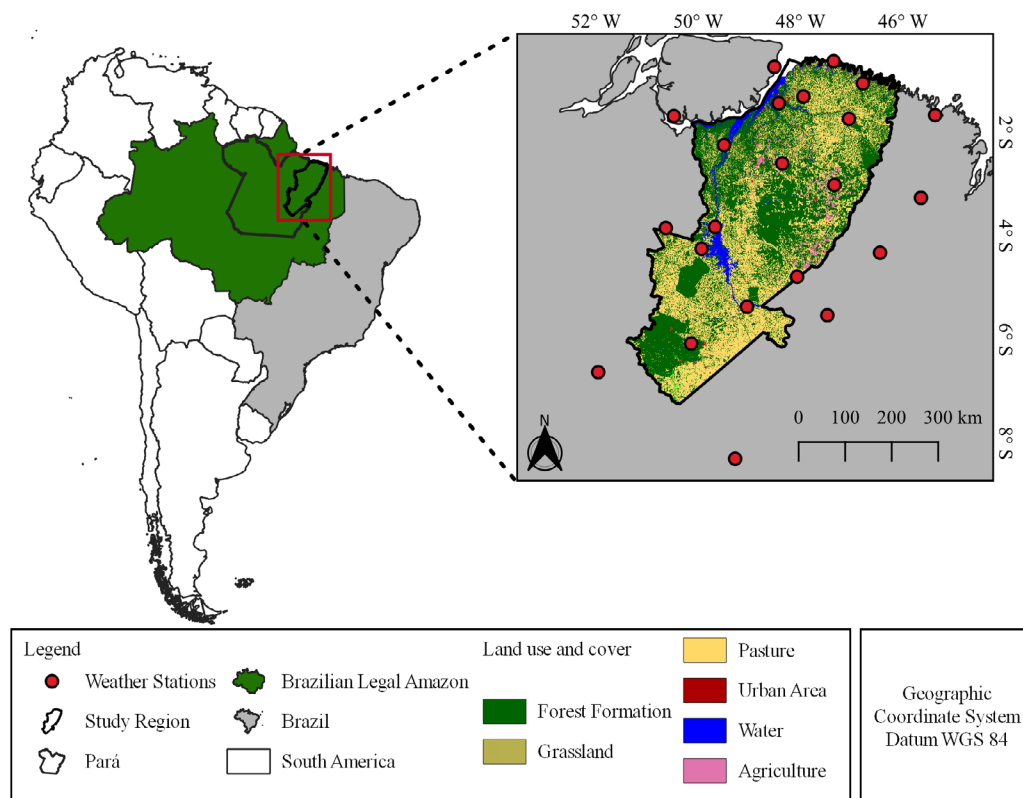
Figure 1. Location and land use map according to MapBiomas (2023) of the studied region, with points showing the position of the weather stations used throughout this study

states. Once the predominant soil texture was determined, the soil water holding capacity was assigned based on the texture, as follows: sandy (80 mm m^{-1}), sandy loam (120 mm m^{-1}), loam (150 mm m^{-1}), clay loam (180 mm m^{-1}), clay (150 mm m^{-1}) for an average root system of 45 cm deep.

The SARRA-H model simulated cowpea sowing, growth, and phenology for each of the 30 stations on the 5th, 15th, and 25th of each month and year, totalizing 36 simulations for weather station and year. The probability of occurrence of the average WRSI greater than or equal to 0.5 during the period that begins with flowering and ends after pod growth was calculated (Andrade Júnior et al., 2007).

Low risk corresponds to 80% or more probability of occurrence of WRSI ≥ 0.5 in the reproductive phase. The moderate climate risk category corresponded to the probability of at least 70% of WRSI ≥ 0.5. And the high risk corresponded to all regions that do not meet the above criteria. The WRSI threshold values for each climate risk class are the same adopted by Andrade Júnior et al. (2007) and Silva et al. (2010).

Based on the discussion raised by Oliveira et al. (2019) about rain events at harvest, EMBRAPA (BRASIL, 2022) defined for cowpea climate risk agricultural zoning 20 mm as the maximum total precipitation tolerable in the ten-day period that encompasses the harvesting of cowpea since excessive rainfall in this period causes irreparable damage to its production (Benchimol et al., 2021).

The risk of rainfall during the harvest period is low when the probability of precipitation < 20 mm during the harvest period is more than 80%, moderate when it is more than 70%, and high when more than 60%. These are the same criteria for the classes of the probability of occurrence of WRSI ≥ 0.5.

Both conditions described above were combined to define the risks for each date and location used. White demarcation identified protected areas.

Coefficient of determination (R^2), agreement index (d), mean error (ME), and root mean square error (RMSE) were used to compare the simulations of leaf biomass, stem biomass, grain yield, total aerial biomass, leaf area index, and soil moisture with the data observed in the field experiments. The calibration procedure used data from the 2013, 2014, and 2015 experiments, while validation used data from the 2016 experiment.

The model evaluation included converting the water content in the soil, as measured by a time domain reflectometer (TDR) (m^3 m^{-3}), into water depth (mm) by taking into account the moisture levels at field capacity (0.252 m^3 m^{-3}) and the permanent wilting point (0.076 m^3 m^{-3}) found during field observations. This result was then multiplied by the soil depth of the water balance conducted in mm. Both simulated and observed data are exclusively related to the surface soil layer (first 30 cm).

Results and Discussion

The SARRA-H model simulates the evolution of the crop's biomass with great precision and accuracy (Table 2). The results for the soil water content have lower accuracy, although satisfactory, in the simulation of treatments L$_2$ and L$_3$. In treatments L$_1$ (control) and L$_4$, both the precision and accuracy of the model were high.

Based on the dry matter of grains (ME), the model overestimated grain yield for L$_1$, L$_2$, and L$_3$ and underestimated it for L$_4$, with overestimates up to 221.76 kg ha^1 (Table 2) on

Table 2. Agreement index (d), determination coefficient (R^2), mean error (ME) and root mean square error (RMSE) for dry matter of shoots, leaves, stems, and grains, leaf area index, and soil moisture during the calibration of the SARRA-H model

Irrigation depth	L_1	L_2	L_3	L_4	L_1	L_2	L_3	L_4
Variable			d				R^2	
Dry matter of shoots	0.99	0.99	0.99	0.99	0.98	0.99	0.98	0.96
Dry matter of leaves	0.96	0.97	0.98	0.94	0.90	0.93	0.95	0.96
Dry matter of stems	0.98	0.99	0.97	0.99	0.95	0.96	0.90	0.95
Dry matter of grains	0.88	0.88	0.90	0.95	0.87	0.89	0.83	0.87
Leaf area index	0.89	0.90	0.84	0.89	0.72	0.72	0.53	0.90
Soil moisture	0.97	0.95	0.87	0.98	0.94	0.82	0.67	0.93
Variable			ME				RMSE	
Dry matter of shoots	-112.11	178.84	209.50	90.87	440.22	499.53	481.27	367.93
Dry matter of leaves	-169.0	-97.14	24.37	130.32	268.95	198.16	164.60	239.38
Dry matter of stems	-138.54	85.90	59.92	-6.39	350.43	288.90	392.45	223.52
Dry matter of grains	221.76	212.68	141.97	-20.53	387.29	361.76	259.98	138.15
Leaf area index	-0.23	-0.12	-0.06	0.18	0.41	0.36	0.43	0.29
Soil moisture	-0.56	-0.89	-2.01	0.51	2.00	2.95	5.24	3.00

L_1 - Irrigation corresponds to 100% of crop evapotranspiration; L_2 - Irrigation corresponds to 50% of crop evapotranspiration; L_3 - Irrigation corresponds to 25% of crop evapotranspiration; and L_4 - No irrigation

average. The model simulations are closer to the measured values during the harvest period (Figure 2). In L_1, the mean grain yield simulated by the model was 1,556 kg ha^1, while the observed yield was 1,338 ± 724 kg ha^1 (mean ± confidence interval, p = 0.05), demonstrating that the simulated yield did not differ statistically from the mean yield observed for this treatment (Figure 2).

Even though the simulated dry matter is not used in the current study, it must be correctly simulated, since the SARRA-H model limits the biomass accumulation based on the ratio of actual (Tr) to potential (TrPot) transpiration. When biomass accumulation is being correctly simulated, it is expected that the model also simulates the effects of water deficit on the crop, and therefore the reduction of transpiration in response to the lack of water in the rootzone. Figure 3 presents the simulation of water stored in the soil during the validation. Except for treatment L_3 (Figure 3C), the temporal variability of water in the soil was simulated with high precision by the model, with emphasis on the water limitation phase when the water consumption of cowpea caused a reduction in water storage throughout the reproductive period.

The model overestimates water consumption between 38 and 55 DAS in L_3 (Figure 3C). The results of the simulation of biomass production (Figure 2C) and the simulation of the soil water content in the other treatments (Figure 3) lead to the conclusion that the model was able to efficiently reproduce this variable, which is of paramount importance for obtaining the WRSI.

Legumes are more susceptible to yield reductions due to drought during flowering than during the vegetative phase (Poudel et al., 2023), because the damage caused to reproductive organs by drought stress can be irreparable.

The climate risk based solely on WRSI is low when sowing is carried out between December (80% of the region) and the end of April (20% of the territory) (Figure 4C). Farmers that sow between the beginning of July and the end of November will likely face the highest climate risk. It makes rainfed production unfeasible in these months.

According to Carvalho et al. (2022), cowpea cultivated in this region tends to have negative impacts on physiological responses and yield when exposed to water deficit during the reproductive stage, presenting a high crop water stress index
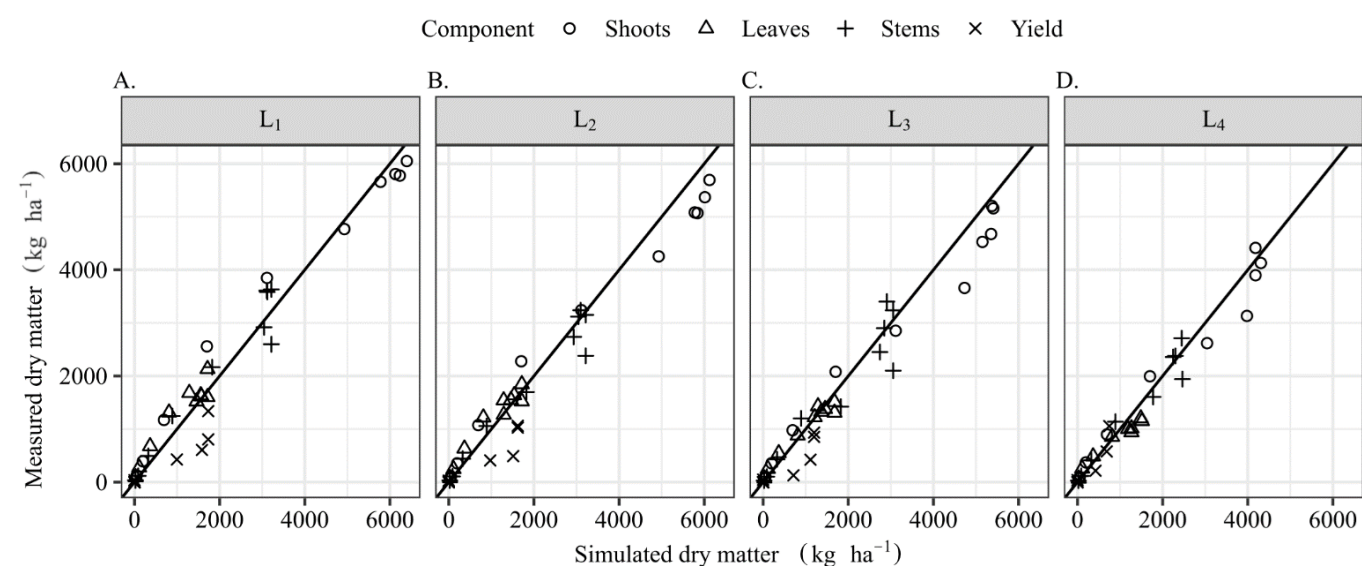

Figure 2. Comparison between measured and simulated dry matter
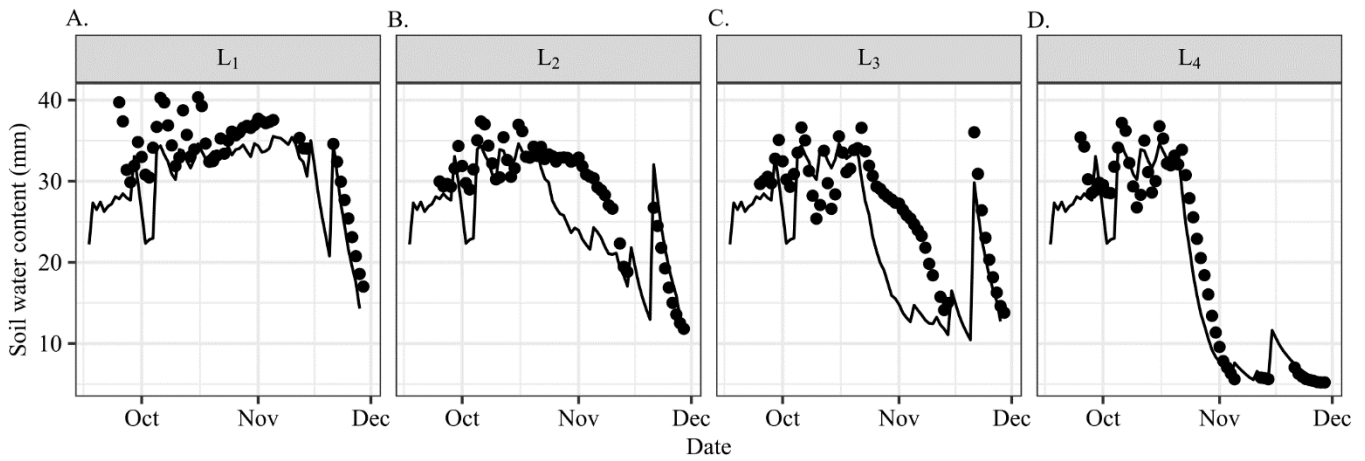
L_1 - Irrigation corresponds to 100% of crop evapotranspiration; L_2 - Irrigation corresponds to 50% of crop evapotranspiration; L_3 - Irrigation corresponds to 25% of crop evapotranspiration; and L_4 - No irrigation

L₁ - Irrigation corresponds to 100% of crop evapotranspiration; L₂ - Irrigation corresponds to 50% of crop evapotranspiration; L₃ - Irrigation corresponds to 25% of crop evapotranspiration; and L₄ - No irrigation

Figure 3. Measured (points) and simulated (lines) soil water content (W - mm) in the surface layer of soil (0-20 cm) under the four irrigation depths
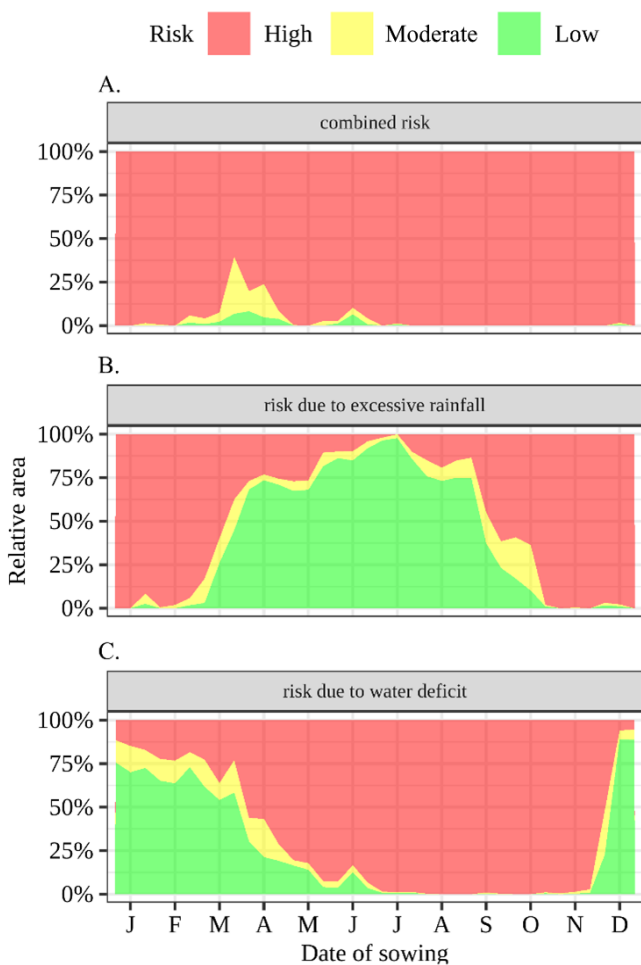
Figure 4. Relative area occupied by each climate risk class (i.e., high, moderate or low risk) throughout the year, in the studied region, as a function of the date of sowing

(CWSI = 0.75) associated with reductions in photosynthetic rate which reach up to 67% at the R8 phenological stage. High CWSIs are related to the presence of water deficit commonly existing in the months shown in Figure 4C (High risk). A strategy to achieve yield higher than the state average (821 kg ha⁻¹) would be to choose periods with CWSI below 0.5 (Carvalho et al., 2022), which coincide with the periods recommended in Figure 4C.

On the other hand, the period that extends from mid-March to the end of September is the most suitable for sowing cowpea in the region, considering the low probability of occurrence of more than 20 mm rainfall depth at the end of the cycle (Figure 4B). Sowing between October and February will lead to high risks due to the frequent rainfalls over the entire studied region.

There are numerous types of fungal diseases that can develop in cowpea, especially in the final harvest phase, some of which are extremely dependent on water shortages (Benchimol et al., 2021). Indicating times of the year with lower risk of rain during the final period of the cycle can avoid significant losses and compromising grain production.

The combination of drought and excessive rainfall risks indicates an ideal period for cowpea sowing that depends on the assessed location (Figure 4A). Less than 10% of the region studied has low risk (80% probability of WRSI ≥ 0.5) when sowing is carried out between March and April or in mid-June, depending on the location in the study area. If a higher risk level is adopted, for example 30%, almost 25% of the region is available for sowings between March and April, and only 15% would be available in June.

From March 15th onwards, the zones of moderate and high climate risk expand in the SE-N direction of the studied region (Figure 5) until mid-June, when only a region on the north remains viable for cultivation, which covers the municipalities of Capanema and Tracuateua, the main producers in the state (Figure 5).

In July the sowing of cowpea in the studied region is practically unfeasible due to limited natural water availability (Figure 5), except for the Metropolitan Mesoregion of Belém, which has low-risk conditions but is not a producing region. The longest sowing window for cowpea production based on the WRSI criteria occurs in the municipalities of Capanema, Tracuateua, and Ipixuna do Pará, which are the largest producers in the state. On the other hand, regions close to 8° S — including the municipality of Santana do Araguaia, which concentrates the second-largest production of cowpea — have an earlier and shorter sowing window, limited to the last ten-day period of March.
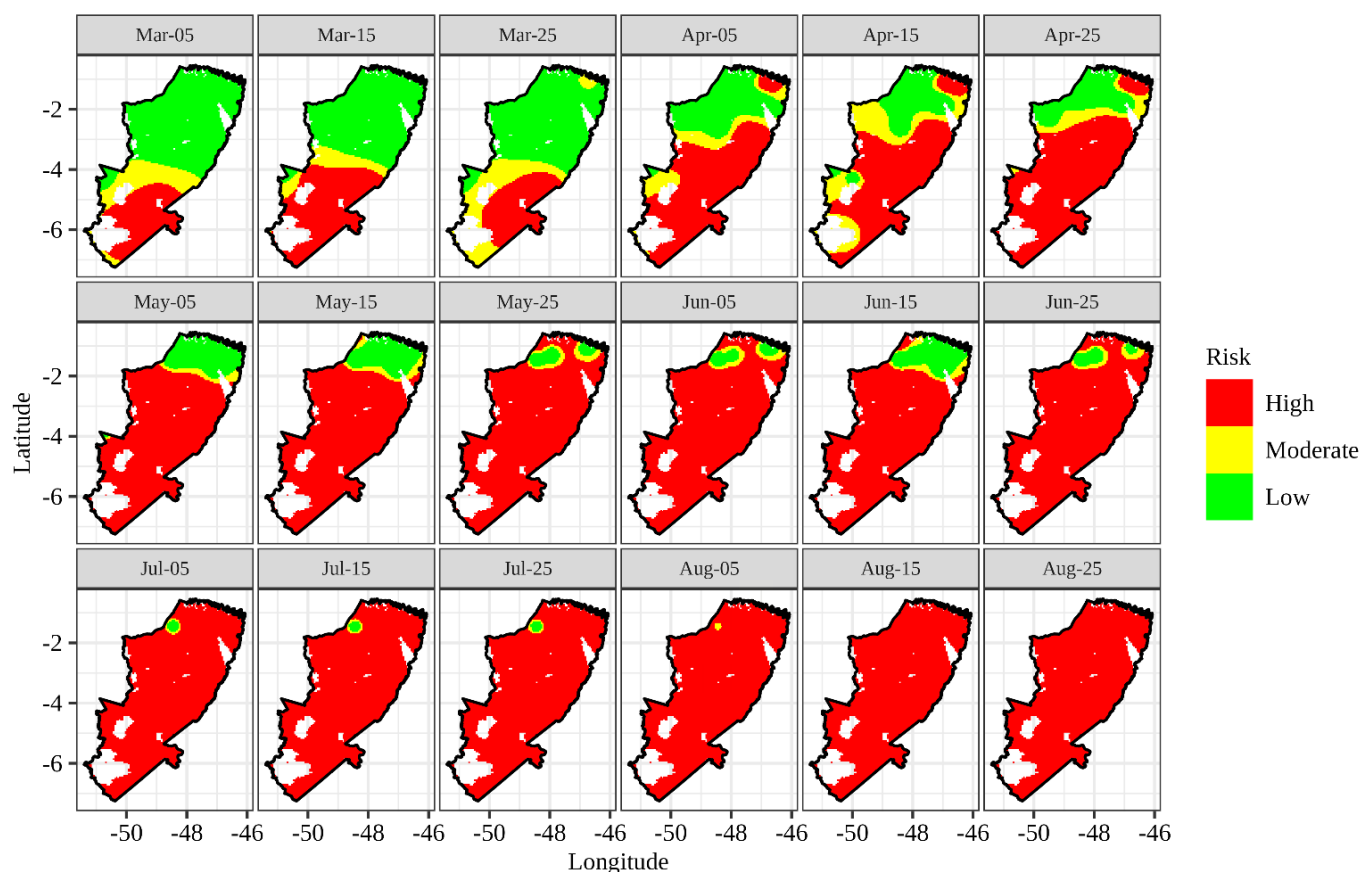
Low risk ≥ 80%; Moderate risk ≥ 70%; High risk < 70% probability of WRSI ≥ 0.5. White areas correspond to protected areas, such as forests and indigenous people's lands

Figure 5. Climate risk classes for different sowing dates of cowpea

The high incidence of rainfall in the northwest of the study region, which led to low climatic risk in this location throughout the entire period (Figure 5), may be associated with the occurrence of squall lines along the coast that propagate westward for distances greater than 400 km, and are responsible for a significant part of the precipitation observed in the region during the first half of the year (Alcântara et al., 2022).

Excessive rainfall throughout fruit development and especially during harvest may impair the yield, as it creates an environment that favors the development of various fungal diseases such as coffee spot, charcoal rot and pod rot (Benchimol et al., 2021) and may have an impact on the development of some insects (Tian et al., 2022) which economically affect production. High soil moisture also increases the incidence of stem rot and damping off caused by *Sclerotium* sp. (Adandonon et al., 2005).

The average duration of the crop cycle, calculated by the SARRA-H model based on the concept of degree-days with the parameters obtained in the experiment (Farias et al., 2015) for the municipalities within the region studied, was 77.9 ± 4.2 days (mean ± standard deviation) for sowings carried out in the last ten days of January and 72.6 ± 3.9 (mean ± standard deviation) days for sowings carried out in the first ten days of September.

Sowing at latitudes lower than 4° S between October and February will likely subject the crop to high accumulated precipitation (Figure 4). The same occurs in regions north of 4° S, with earlier sowing. The risk of rainfall above 20 mm at the end of the cycle is low (probability below 20%) in the region located at latitudes north of 2° S from April onwards (Figure 6).

Between March and May, in regions closer to the equator, and from July onwards, for locations south of 6° S, the risk of rainfall exceeding 20 mm at harvest is greater than 40% (Figure 6) due to onset of the wet season. Studies on the risk of rainfall at harvest for this region offer better decision-making power to local farmers regarding the best sowing dates within the recommended sowing window. It allows analysts to exclude periods with high humidity, which increases the spread of diseases (Benchimol et al., 2021).

With the inclusion of the rainfall criteria, the sowing window corresponds to late May and late June (Figure 7). Sowing earlier or later will subject the crop to a high probability of rainfall at harvest or water deficit in the grain-growth phase.

The region located between the 2° and 8° S parallels, which extends from the municipality of Santana do Araguaia (second largest producer) in the south up to Ipixuna do Pará (fourth largest producer) in the north, has a short sowing window, which corresponds to the last ten days of March. Sowing can be carried out after March in regions between 2° and 3° S and between 4° and 8° S with moderate risk (Figure 7). From May onwards, sowing north of 2° S becomes risky due to insufficient rainwater during the growth and development of the crop.

The displacement of the intertropical convergence zone (ITCZ), which advances towards the northern hemisphere (Kousky & Molion, 1985) at the beginning of the second half of the year, explains the rapid increase of the climate risk in most of the region at the end of the wet season. The ITCZ is the primary rain-generating system in Eastern Amazon during the wet season, notably in Maranhão state and northeastern
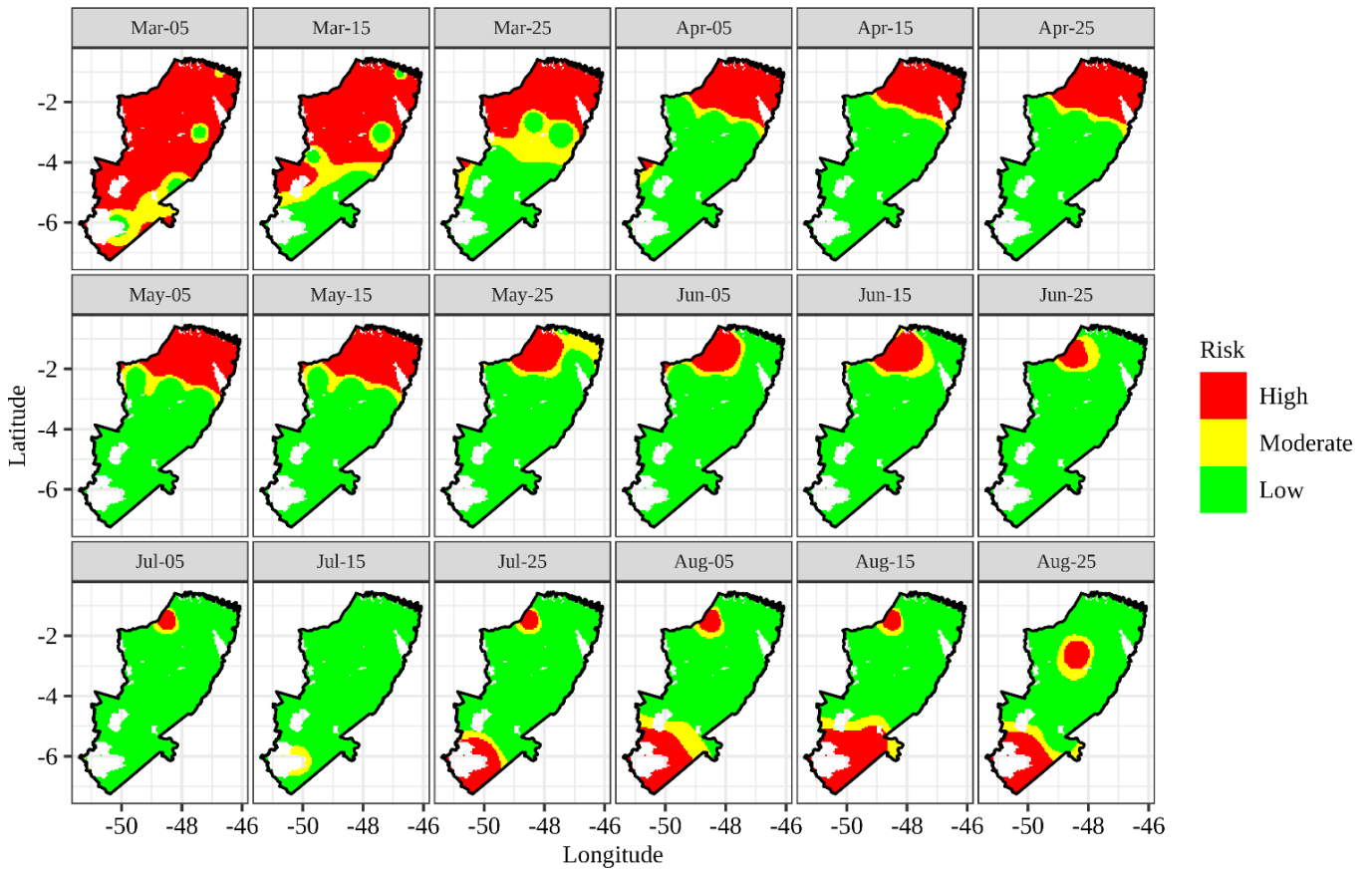
Low ≥ 80%; Moderate ≥ 70%; High < 70% probability of rain at harvest ≤ 20 mm. Blank areas correspond to protected areas

Figure 6. Climate risk classes for different sowing dates of cowpea
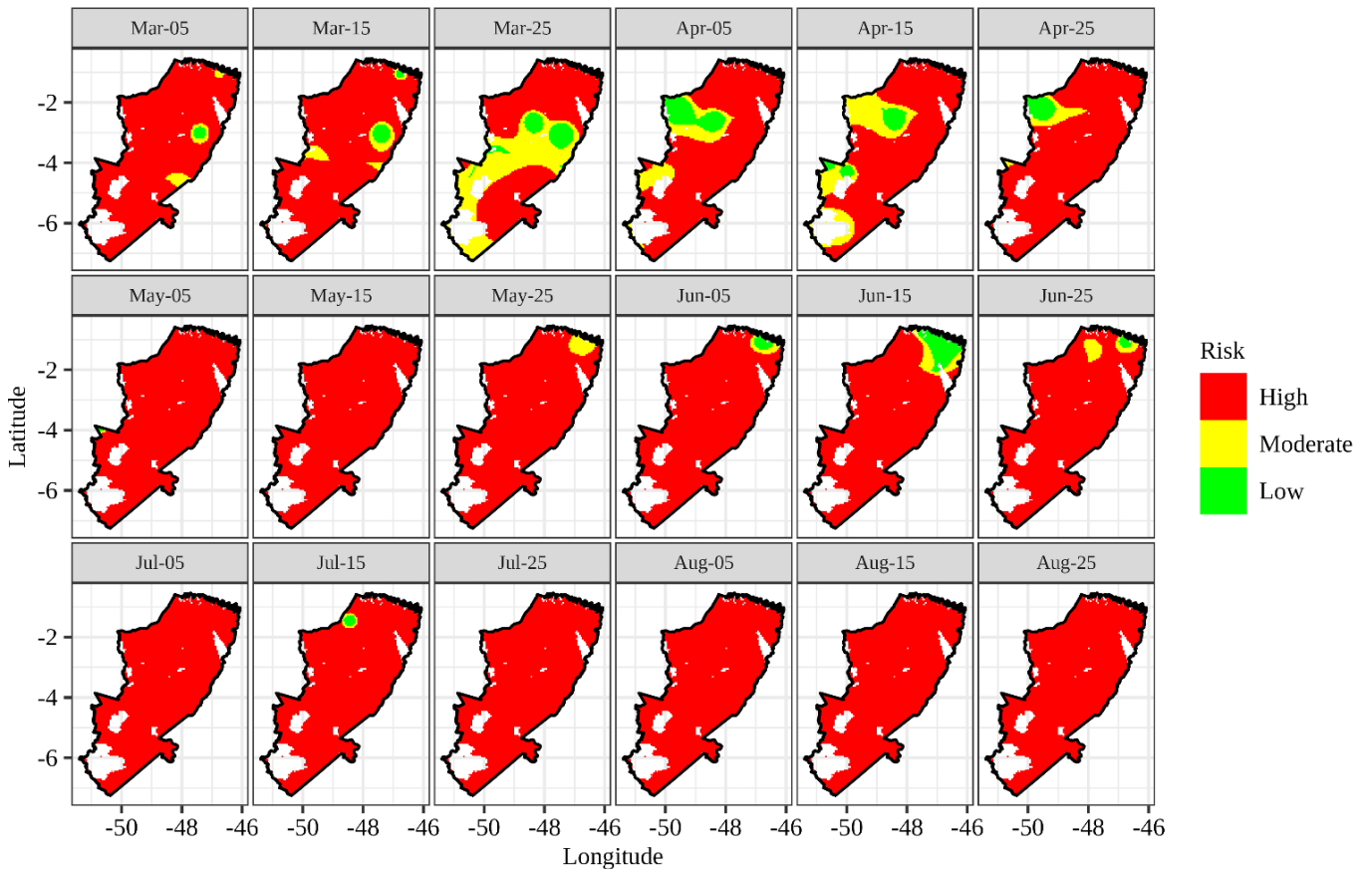
Low ≥ 80%; Moderate ≥ 70%; Low < 70% probability of rain at harvest ≤ 20 mm. Blank areas correspond to protected areas

Figure 7. Combined climate risk classes for different sowing dates of cowpea

Table 3. Sowing window for different locations in the northeast of the state of Pará, depending on latitude, based on the combination of WRSI and risk of rain at harvest, according to simulation results by the SARRA-H model

Latitude	March			April			May			June			July			August		
Ten-day period	1st	2nd	3rd	1st	2nd	3rd	1st	2nd	3rd	1st	2nd	3rd	1st	2nd	3rd	1st	2nd	3rd
0° - 2° S									▓	▓	▓	▓						
2° S - 4° S				▓	▓	▓												
4° S - 8° S			▓															

of Pará state (Aguiar et al., 2022). Furthermore, an annual seasonal shift of the convective activity associated with the displacement of the ITCZ occurs in the N-SE direction, which increases precipitation over the Amazon in the first quarter of the year and, subsequently, increases the precipitation over Central America in the third quarter (Ferreira et al., 2015).

The movement of the low climate risk zone along the SE-N direction from March to June is associated with the amount and distribution of the annual precipitation at the north and south of the studied region. Carvalho et al. (2020) show a clear difference between both regions regarding the dry season, which extends from June to September in Marabá (located further south) and from September to November in Tracuateua (located further north), a difference that may explain why the period of low climate risk ends later in the northern locations.

By combining the WRSI criteria and the probability of rain at harvesting, one can notice that the sowing window in the region comprised between the parallels 0° and 2° S extends from late May to late June, with mid-June being the best period. The sowing window between 2° and 4° S is limited to the first 20 days of April, and between 4° and 8° S it is limited to late March (Table 3).

The sowing window in the studied region is shorter than that defined in other studies conducted in Brazil that considered only the WRSI criteria. Andrade Júnior et al. (2007) proposed mid-October to late March as the most suitable period for sowing cowpea in the state of Ceará, Brazil. Lima Filho et al. (2013) defined the period from mid-June to mid-July for Cruz das Almas in the Recôncavo Baiano, Brazil. However, precipitation in these locations is much lower than in northeastern Pará, which may significantly reduce the risk of rainfall at harvest, expanding the sowing window in these regions.

The indication of risk based on the combined presence of water deficit in the reproductive phase and rain at harvest is a significant advance but is still not ideal and definitive information. According to Battisti & Sentelhas (2014), an approach that allows an analysis of the yield obtained and the cost of production would be additional information that would actually define the best time to plant a crop.

Simulations carried out with the Aquacrop model (Nunes et al., 2019), without however considering the effect of rain at harvest, indicate an optimal sowing window (OSW) for cowpea in the region that runs from January to May with attainable yield values close to the average values for potential yield (1,610 kg ha^{-1}). For the period recommended in climatic risk zoning (1st, 2nd, and 3rd ten-day periods of June), the attainable yield corresponds to approximately 1,330, 1,290 and 1,200 kg ha^{-1}.

A narrow window is established to produce cowpea in the major producing regions of Pará due to the local precipitation regime, which is typical of an Am climate (Alvares et al., 2014), with a well-defined rainy season in the 1st half of the year and

less rainy season in the 2nd half. Adopting no-tillage at the end of the sowing window may contribute to its expansion due to the increased retention of water in the soil with such practices (Andrade Júnior et al., 2018).

Another alternative would be the use of supplementary irrigation to extend the window after the end of June, ensuring a low risk of rain at harvest (Figure 6) and yields close to the potential yield that tend to increase with late planting (Nunes et al., 2019) since there can be a gain of around 16 to 17 bags ha^{-1} in yield and an increase in gross revenue between US\$711 and US\$867 due to the use of irrigation in the reproductive phase (Carvalho et al., 2023).

Conclusions

1. The SARRA-H model was able to simulate cowpea growth and development as well as the soil water balance after its calibration.

2. The region under study has a low climatic risk for sowing cowpea between March and June considering the probability of water deficit during reproductive stage and several rain events during the harvest period.

3. In the region closer to the equator a later sowing window can be adopted.

Literature Cited

Adandonon, A.; Avelin, T. A. S.; Labuschagne, N.; Ahohuendo, B. C. Etiology of and effect of environmental factors on damping-off and stem rot of cowpea in Benin. Phytoparasitica, v.33, p.65-72, 2005. https://doi.org/10.1007/BF02980927

Aguiar, A. L.; Marta-Almeida, M.; Cruz, L. O.; Pereira, J.; Cirano, M. Forcing mechanisms of the circulation on the Brazilian Equatorial Shelf. Continental Shelf Research, v.247, p.1-17, 2022. https://doi.org/10.1016/j.csr.2022.104811

Alcântara, C. R.; Carneiro, I. O.; Oliveira, G. B. Analysis of meteorological variables interaction associated with the environment of formation of Amazonian squall lines. Anais da Academia Brasileira de Ciencias, v.94, p.1-18, 2022. https://doi.org/10.1590/0001-3765202220201739

Allen, R. G.; Pereira, L. S.; Howell, T. A.; Jensen, M. E. Evapotranspiration information reporting: I. Factors governing measurement accuracy. Agricultural Water Management, v.98, p.899-920, 2011. https://doi.org/10.1016/j.agwat.2010.12.015

Alvares, C. A.; Stape, J. L.; Sentelhas, P. C.; Gonçalves, J. L. de M.; Sparovek, G. Köppen's climate classification map for Brazil. Meteorologische Zeitschrif, v.22, p.711-728, 2014. https://doi.org/10.1127/0941-2948/2013/0507

Andrade Júnior, A. S. de; Bastos, E. A.; Silva, M. V. P. da; Silva Junior, J. S. da; Monteiro, J. E. B. de A. Índice de satisfação da necessidade de água do feijão-caupi sob sistema de cultivo convencional e plantio direto. Revista Agrometeoros, v.26, p.201-211, 2018.

Andrade Júnior, A. S. de; Freire-Filho, F. R.; Barros, A. H. C.; Silva, C. O. da. Zoneamento de risco climático para a cultura do feijão-caupi no Estado do Ceará. Revista Ciência Agronômica, v.38, p.109-117, 2007.

Battisti, R.; Sentelhas, P. C. New agroclimatic approach for soybean sowing dates recommendation: A case study. Revista Brasileira de Engenharia Agrícola e Ambiental, v.18, p.1149-1156, 2014. http://dx.doi.org/10.1590/1807-1929/agriambi.v18n11p1149-1156

Benchimol, R. L.; Freire Filho, F. R.; Gomes Junior, R. A.; Rodrigues, J. E. L.; Silva, C. M. da; Cardoso, R. S.; Rosário, R. G. A. do. Doenças fúngicas do feijão-caupi no estado do Pará. Belém: Embrapa Amazônia oriental, 2021. 31p.

BRASIL. Portaria SPA/MAPA nº 67 de 26 de abril de 2022. Aprova o Zoneamento Agrícola de Risco Climático - ZARC para a cultura do Feijão Caupi no Estado do Pará, ano-safra 2022/2023. In: Diário Oficial da União, seção 1. Brasília, DF: Imprensa Oficial, 2022. Available on: https://www.gov.br/agricultura/pt-br/assuntos/riscos-seguro/programa-nacional-de-zoneamento-agricola-de-risco-climatico/portarias/2022-2023/para-pa/port-no-67-feijao-caupi-pa-ret.pdf. Accessed on: Oct. 2023.

Carvalho, E. de O. T. de; Costa, D. L. P.; Vieira, I. C. de O.; Ferreira, B. G.; Nunes, H. G. G. C.; Souza, P. J. de O. P. de. Crop water stress index of cowpea under different water availability levels in Castanhal-PA. Revista Caatinga, v.35, p.711-721, 2022. https://doi.org/10.1590/1983-21252022v35n322rc

Carvalho, E. de O. T. de; Costa, D. L. P.; Luz, D. B.; Rua, M. L.; Velame, M. L. A.; Monteiro, A. C.; Vieira, I. C. O.; Pinto, J. V. N.; Fernandes, G. S. T.; Nunes, H. G. G. C.; Souza, P. J. de O. P. de; Santos, M. A. S. Revista Brasileira de Engenharia Agrícola e Ambiental, v.27, p.618-624, 2023. http://dx.doi.org/10.1590/1807-1929/agriambi.v27n8p618-624

Carvalho, S.; Oliveira, A.; Pedersen, J. S.; Manhice, H.; Lisboa, F.; Norguet, J.; Wit, F. de; Santos, F. D. A changing Amazon rainforest: Historical trends and future projections under post-Paris climate scenarios. Global and Planetary Change, v.195, p.1-13, 2020. https://doi.org/10.1016/j.gloplacha.2020.103328

CIRAD - Centre de coopération internationale en recherche agronomique pour le développement. SARRA-H Modèle de culture, 2023. Available on: <https://sarra-h.teledetection.fr>. Accessed on: Sep. 2023.

Farias, V. D. da S.; Costa, D. L. P.; Souza, P. J. de O. P.; Takaki, A. Y.; Lima, M. J. A. Temperaturas basais e necessidade térmica para o ciclo do feijão caupi. Enciclopédia Biosfera, v.11, p.1781-1792, 2015.

Farias, V. D. da S.; Lima, M. J. A. de; Nunes, H. G. G. C.; Sousa, D. de P.; Souza P. J. de O. P. de. Water demand, crop coefficient and uncoupling factor of cowpea in the eastern Amazon. Revista Caatinga, v.30, p.190-200, 2017. https://doi.org/10.1590/1983-21252017v30n121rc

Ferreira DBS, De Souza EB, De Moraes BC, Meira Filho LG (2015) Spatial and temporal variability of rainfall in Eastern Amazon during the rainy season. Scientific World Journal, v.2015, p.1-9, 2015. https://doi.org/10.1155/2015/209783

Kousky, V. E.; Molion, L. C. Uma contribuição a climatologia da dinâmica da troposfera sobre a Amazônia. Acta Amazônica, v.15, p.311-320, 1985. https://doi.org/10.1590/1809-43921985153320

Lima Filho, A. F.; Coelho Filho, M. A.; Heinemann, A. B. Determinação de épocas de semeadura do feijão caupi no Recôncavo Baiano através do modelo CROPGRO. Revista Brasileira de Engenharia Agrícola e Ambiental, v.17, p.1294-1300, 2013. https://doi.org/10.1590/S1415-43662013001200007

Machado, C. de F.; Teixeira, N. J. P.; Freire Filho, F. R.; Rocha, M. de M.; Gomes, R. L. F. Identificação de genótipos de feijão-caupi quanto à precocidade, arquitetura da planta e produtividade de grãos. Revista Ciência Agronômica, v.39, p.114-123, 2008.

MAPBIOMAS. Plataforma MapBiomas Brasil, 2023. Available on: https://brasil.mapbiomas.org/en/. Accessed on: Sep. 2023.

Nunes, H. G. G. C.; Sousa, D. de P.; Moura, V. B.; Ferreira, D. P.; Pinto, J. V. de N.; Vieira, I. C. de O.; Farias, V. D. da S.; Oliveira, E. C. de; Souza, P. J. O. P. de. Performance of the AquaCrop model in the climate risk analysis and yield prediction of cowpea (*Vigna unguiculatta* L.Walp). Australian Journal of Crop Science, v.13, p.1105-1112, 2019. https://doi.org/10.21475/ajcs.19.13.07.p1590

Oliveira, I. J.; Fontes, J. R. A.; Dias, M. C.; Barreto, J. F. Recomendações técnicas para o cultivo do feijão-caupi no estado Amazonas. Manaus: Embrapa Amazônia oriental, 2019. 30p. Embrapa Amazônia Ocidental. Circular Técnica, 71

Poudel, S.; Vennam, R. R.; Shrestha, A.; Reddy, K. R.; Wijewardane, N. K.; Reddy, K. N.; Bheemanahalli, R. Resilience of soybean cultivars to drought stress during flowering and early-seed setting stages. Scientific Reports, v.13, p.1-13, 2023. https://doi.org/10.1038/s41598-023-28354-0

Silva, V. de P. R.; Campos, J. H. B. C.; Silva, M. T.; Azevedo, P. V. Impact of global warming on cowpea bean cultivation in northeastern Brazil. Agricultural Water Management, v.97, p.1760-1768, 2010. https://doi.org/10.1016/j.agwat.2010.06.006

Sousa , D. de P.; Nunes, H. G. G. C.; Ferreira, D. P.; Moura, V. B.; Aviz, W. L. C. de; Santos, H. C. A.; Pinto, J. V. de N.; Vieira, I. C. de O.; Fernandes, G. S. T.; Silva, E. R. R.; Belém, L. T.; Cunha Junior, J. B. da; Lima, M. J. A. de; Sousa, A. M. L.; Farias, V. D. S. da; Santos, J. T. S.; Souza, P. J.de O. P. de. Performance of Cowpea under Different Water Regimes in Amazonian Conditions. Horticulturae, v.8, p.1-12, 2022. https://doi.org/10.3390/horticulturae8040335

Sousa, D. de P.; Souza, P. J. O. P. de; Farias, V. D. da S.; Nunes, H. G. G. C.; Ferreira, D. P.; Pinto, J. V. N.; Lima, M. J. A. de. Radiation Use Efficiency for Cowpea Subjected to Different Irrigation Depths Under the Climatic Conditions of the Northeast of Pará State. Revista Brasileira de Meteorologia, v.33, p.579-587, 2018. https://doi.org/10.1590/0102-7786334001

Souza, P. J. de O. P.; Farias, V. D. da S., Pinto, J. V. N. P., Nunes, H. G. G. C., Souza, E. B. de; Fraisse, C. W. Yield gap in cowpea plants as function of water deficits during reproductive stage. Revista Brasileira de Engenharia Agrícola e Ambiental, v.24, p.1-12, 2020. https://doi.org/10.1590/1807-1929/agriambi.v24n6p372-378

Tian, T.; Ren, Q.; Fan, J.; Haseeb, M.; Zhang, R. Too dry or too wet soils have a negative impact on larval pupation of fall armyworm. Journal of Applied Entomology, v.146, p.196-202, 2022. https://doi.org/10.1111/jen.12950

Yang, M.; Wang, G.; Wu, S.; Block, P.; Lazin, R.; Alexander, S.; Lala, J.; Haider, M. R.; Dokou, Z.; Atsbeha, E. A.; Koukoula, M.; Shen, X. Seasonal prediction of crop yields in Ethiopia using an analog approach. Agricultural and Forest Meteorology, v.331, p.1-11, 2023. https://doi.org/10.1016/j.agrformet.2023.109347